

An Effective Use of Radio Altimeter to GPS/DME Integration System

Moonsuk Koo

Department of Electronics Engineering/Chungnam National University/Korea
+82-42-821-7709 & +82-42-823-5436, koomoonsuk@cnu.ac.kr

Sun Yong Lee

Department of Electronics Engineering/Chungnam National University/Korea
+82-42-821-7706 & +82-42-823-5436, sy_lee@cnu.ac.kr

Hyoungmin So

3-4/Agency for Defence Development/Korea
+82-42-821-4463, hmso@add.re.kr

Sang Heon Oh

Integrated Navigation Division/Navcours Co., Ltd./Korea
+82-42-363-9249 & +82-42-363-9240, laborosh@navcours.com

Dong-Hwan Hwang

Department of Electronics Engineering/Chungnam National University/Korea
+82-42-821-5670 & +82-42-823-5436, dhhwang@cnu.ac.kr

Sang Jeong Lee

Department of Electronics Engineering/Chungnam National University/Korea
+82-42-821-6582 & +82-42-823-4494, eesjl@cnu.ac.kr

ABSTRACT

In order to overcome vulnerability of GNSS, lots of researches on use of ground navigation systems have been found. An effective use of an altimeter is proposed in an integration of GNSS/DME integration system. A weighted DOP which is based on statistics of measurement error, is derived for a given vehicle motion trajectory. From the derived DOP, the vertical error is estimated. By comparing the estimated vertical error with error specification of the altimeter, use of the altimeter is determined in the integrated navigation system. In order to show efficiency of the proposed method, 50 times Monte-Carlo simulations were performed for a GPS/DME integrated navigation system.

KEYWORDS: GNSS, Ground Navigation, Integrated Navigation, Altimeter, DOP

1. INTRODUCTION

Accurate altitude information is essential for safe operation in aircrafts. Especially when an aircraft is over the ground with complex features rather than the sea, it is required to get a method to acquire reliable altitude information for safety. INS (Inertial Navigation System),

altimeter, and GNSS (Global Navigation Satellite System) can provide aircrafts with altitude information. Even though the INS can provide quite accurate altitude information in a comparatively short time, the altitude error diverges as time progresses even when an IMU (Inertial Measurement Unit) with high performance is used (Titterton and Weston, 2004). As a result of this, combined use of a barometric altimeter and/or a radio altimeter with INS has been proposed in order to avoid divergence of the altitude error of the INS (Blanchard, 1971, Kayton and Fried, 1997). The radio altimeter is usually equipped in the military aircrafts and measures AGL (Above Ground Level) by sending a pulse to the ground and receiving reflected signal. Even though the radio altimeter gives a comparatively accurate altitude output in low altitude, it gives highly inaccurate output as the altitude increases due to the attenuation of the radio signal intensity (Waite and Schmidt, 1962, Yoon *et al.*, 2013).

GNSS can provide a horizontal navigation output as well as altitude output when the number of visible satellites are enough. GNSS navigation accuracy depends on pseudo-range measurement error and DOP (Dilution of Precision) which represent a characteristic of the geometric arrangement of the satellites. In general, the altitude error of GNSS is known to have 1.5 times of the horizontal error. In order to have 3-dimensional position and time, more than four GNSS measurements should be acquired (Perrotta *et al.*, 1997). Cases may occur that navigation cannot be performed since enough measurements are not available in intentional or unintentional jamming environment (Bevly and Cobb, 2008, Misra and Enge, 2006). Therefore, in order to compensate this vulnerability of the GNSS, lots of researches on using GNSS and ground based radio navigation systems have been proposed (FAA, 2014).

Among the ground based radio navigation systems, DME (Distance Measuring Equipment) is a pulse ranging system using principle of the radar to have range information between aircraft and ground station (Gebre-Egziabher, 2004). The DME interrogator which is equipped in the aircraft sends pulse signal in the UHF band to the DME ground station. Once the pulse signal from aircraft's interrogator is received in the DME ground station, the DME transponder resends pulse signal after 50 μ s delay. The slant range to the DME ground station can be acquired in the aircraft from difference between time consumed in the transmission and reception and 50 μ s of delay time.

Since the DME station is on the ground, the DME has a very large VDOP (Vertical DOP) compared to GNSS and cannot provide an accurate altitude information when DME alone is used. Therefore, if the DME slant range measurement and GNSS pseudo-range measurement are combined, continuous navigation solutions as well as altitude information can be obtained even when the number of pseudo-range measurements is less than four. However, accuracy of the altitude information depends on the altitude of the vehicle and geometry of GNSS satellites even in this case. In order to compensate this disadvantage, more accurate navigation information can be provided when information of the radio altimeter is used appropriately.

In this paper, an effective use of radio altimeter in the GPS/DME integration system is proposed. In section 2, a GPS/DME integration algorithm using the WLSM (Weighted Least Square Method) is described. In section 3, an effective use of radio altimeter in the GPS/DME integration system using the WDOP (Weighted DOP) is described. In section 4, effectiveness of the proposed method is shown through simulation, and concluding remarks and further study are given in the last section.

2. GPS/DME INTEGRATION ALGORITHM USING WEIGHTED LEAST SQUARE METHOD

The GPS navigation algorithm using least square method is described in detail in many literatures (Kaplan and Hegarty, 2005, Leick, 1995, Hofmann-Wellenhof *et al.*, 1994). The GPS measurement model is represented in equation (1) ~ (4).

$$\mathbf{H}_G \Delta \hat{\mathbf{x}}_G = \Delta \hat{\boldsymbol{\rho}}_G \quad (1)$$

$$\Delta \hat{\mathbf{x}}_G = \mathbf{x}_{G_T} - \mathbf{x}_{G_L} + d\mathbf{x}_G = \begin{bmatrix} \Delta \hat{\rho}_N & \Delta \hat{\rho}_E & \Delta \hat{\rho}_D & c\Delta \hat{b} \end{bmatrix}^T \quad (2)$$

$$\Delta \hat{\boldsymbol{\rho}}_G = \boldsymbol{\rho}_{G_T} - \boldsymbol{\rho}_{G_L} + d\boldsymbol{\rho}_G \quad (3)$$

$$\mathbf{H}_G = \begin{bmatrix} \mathbf{a}_1^T & 1 \\ \mathbf{a}_2^T & 1 \\ \vdots & 1 \\ \mathbf{a}_n^T & 1 \end{bmatrix} = \begin{bmatrix} a_{x1} & a_{y1} & a_{z1} & 1 \\ a_{x2} & a_{y2} & a_{z2} & 1 \\ \vdots & \vdots & \vdots & \vdots \\ a_{xn} & a_{yn} & a_{zn} & 1 \end{bmatrix} \quad (4)$$

where $\Delta \hat{\mathbf{x}}_G$ denotes estimated position and clock bias offset, \mathbf{x}_{G_T} true user position and time, \mathbf{x}_{G_L} position and time defined as the linearization point, and $d\mathbf{x}_{G_L}$ position and time error. $\Delta \hat{\rho}_{N,E,D}$ denotes estimated north, east, and down position offset and $\Delta \hat{b}$ estimated clock bias offset. c denotes speed of light. $\Delta \hat{\rho}_{G_T}$ denotes pseudo-range offset with error, $\boldsymbol{\rho}_{G_T}$ true pseudo-range measured at the true user position, $\boldsymbol{\rho}_{G_L}$ pseudo-range computed at the linearization point, and $d\boldsymbol{\rho}_{G_L}$ pseudo-range error. \mathbf{a}_i denotes unit vector pointing from the linearization point to the location of the i -th satellite and n denotes number of GPS observations.

Position of the vehicle $\hat{\mathbf{x}}_{G_U}$ can be obtained as equation (5) and (6) from GPS measurements.

$$\Delta \hat{\mathbf{x}}_G = (\mathbf{H}_G^T \mathbf{H}_G)^{-1} \mathbf{H}_G^T \Delta \hat{\boldsymbol{\rho}}_G \quad (5)$$

$$\hat{\mathbf{x}}_{G_U} = \mathbf{x}_{G_L} + \Delta \hat{\mathbf{x}}_G \quad (6)$$

Position determination of the vehicle using DME measurements can also be performed as the same method as the GPS navigation algorithm. In this case, the clock bias variable is excluded. Equation (7) ~ (10) represents DME measurement model.

$$\mathbf{H}_D \Delta \hat{\mathbf{x}}_D = \Delta \hat{\boldsymbol{\rho}}_D \quad (7)$$

$$\Delta \hat{\mathbf{x}}_D = \mathbf{x}_{D_T} - \mathbf{x}_{D_L} + d\mathbf{x}_D = \begin{bmatrix} \Delta \hat{\rho}_N & \Delta \hat{\rho}_E & \Delta \hat{\rho}_D \end{bmatrix}^T \quad (8)$$

$$\Delta \hat{\boldsymbol{\rho}}_D = \boldsymbol{\rho}_{D_T} - \boldsymbol{\rho}_{D_L} + d\boldsymbol{\rho}_D \quad (9)$$

$$\mathbf{H}_D = \begin{bmatrix} \mathbf{b}_1^T \\ \mathbf{b}_2^T \\ \vdots \\ \mathbf{b}_m^T \end{bmatrix} = \begin{bmatrix} b_{x1} & b_{y1} & b_{z1} \\ b_{x2} & b_{y2} & b_{z2} \\ \vdots & \vdots & \vdots \\ b_{xm} & b_{ym} & b_{zm} \end{bmatrix} \quad (10)$$

where $\Delta\hat{\mathbf{x}}_D$ denotes estimated position offset, \mathbf{x}_{D_T} true user position, \mathbf{x}_{D_L} position and time defined as the linearization point, and $d\mathbf{x}_{D_L}$ position error. $\Delta\hat{\boldsymbol{\rho}}_{D_T}$ denotes slant range offset with error, $\boldsymbol{\rho}_{D_T}$ true pseudo-range measured at the true user position, $\boldsymbol{\rho}_{D_L}$ slant range computed at the linearization point, and $d\boldsymbol{\rho}_{D_L}$ slant range error. \mathbf{b}_i denotes unit vector pointing from the linearization point to the location of the i -th DME station. m denotes number of DME observations.

Position of the vehicle $\hat{\mathbf{x}}_{D_V}$ can be obtained as equation (11) and (12).

$$\Delta\hat{\mathbf{x}}_D = (\mathbf{H}_D^T \mathbf{H}_D)^{-1} \mathbf{H}_D^T \Delta\hat{\boldsymbol{\rho}}_D \quad (11)$$

$$\hat{\mathbf{x}}_{D_V} = \mathbf{x}_{D_L} + \Delta\hat{\mathbf{x}}_D \quad (12)$$

Since magnitude of the DME measurement error is different from that of the GPS measurement error, the GPS/DME integrated navigation algorithm uses the WLSM which considers error specification of each system. The measurement model of the GPS/DME integration system is given in equation (13) ~ (16).

$$\mathbf{H}\Delta\hat{\mathbf{x}} = \Delta\hat{\boldsymbol{\rho}} \quad (13)$$

$$\Delta\hat{\mathbf{x}} = [\Delta\hat{\rho}_N \quad \Delta\hat{\rho}_E \quad \Delta\hat{\rho}_D \quad c\Delta\hat{b}]^T \quad (14)$$

$$\Delta\hat{\boldsymbol{\rho}} = [\Delta\hat{\boldsymbol{\rho}}_G \quad \Delta\hat{\boldsymbol{\rho}}_D]^T \quad (15)$$

$$\mathbf{H} = \begin{bmatrix} \mathbf{H}_G \\ \mathbf{H}_D \quad \mathbf{0}_{m \times 1} \end{bmatrix} \quad (16)$$

Position of the vehicle can be obtained as equation (17) ~ (21) from GPS and DME measurements using the WLSM (Kaplan and Hegarty, 2005, Langley, 1999).

$$\Delta\hat{\mathbf{x}} = (\mathbf{H}^T \mathbf{W} \mathbf{H})^{-1} \mathbf{H}^T \mathbf{W} \Delta\hat{\boldsymbol{\rho}} \quad (17)$$

$$\mathbf{W} = \mathbf{R}^{-1} \quad (18)$$

$$\mathbf{R} = \begin{bmatrix} \mathbf{R}_G & \mathbf{0}_{m \times m} \\ \mathbf{0}_{n \times n} & \mathbf{R}_D \end{bmatrix} \quad (19)$$

$$\mathbf{R}_G = \begin{bmatrix} \sigma_{G1}^2 & \cdots & 0 \\ \vdots & \ddots & \vdots \\ 0 & \cdots & \sigma_{Gn}^2 \end{bmatrix} \quad (20)$$

$$\mathbf{R}_D = \begin{bmatrix} \sigma_{D1}^2 & \cdots & 0 \\ \vdots & \ddots & \vdots \\ 0 & \cdots & \sigma_{Dm}^2 \end{bmatrix} \quad (21)$$

where \mathbf{W} denotes weighting matrix and σ_{Gi}^2 denotes pseudo-range error variance of the i -th GPS satellite. \mathbf{R}_G denotes pseudo-range error covariance matrix and σ_{Di}^2 denotes slant range error variance of the i -th DME station. \mathbf{R}_D denotes slant range error covariance matrix.

3. EFFECTIVE USE OF RADIO ALTIMETER USING WDOP

Accuracy of the position in the GPS/DME integration system is determined from measurement error and geometry of GNSS satellites and DME stations. The DOP increases when the GPS measurements are not enough due to jamming. Since the DME station is on the ground, the altitude error is very large when the altitude is low. Therefore, when altitude output of the GPS/DME integration system is not accurate enough, use of a radio altimeter can be considered. However, since error of the radio altimeter increases as altitude of the vehicle becomes higher, a method is needed to select more accurate altitude information between the output of the radio altimeter and that of the GPS/DME integration system in order to use the altitude information of the radio altimeter more effectively.

When each measurement has an identical error characteristic in the GPS/DME integration system, that is, $\sigma_G^2 = \sigma_{G1}^2 = \dots = \sigma_{Gn}^2$, $\sigma_D^2 = \sigma_{D1}^2 = \dots = \sigma_{Dm}^2$, the weighting matrix in equation (17) can be represented in equation (22) using variance of the GPS measurement.

$$\begin{aligned} \mathbf{W} = \mathbf{R}^{-1} &= \begin{bmatrix} \frac{1}{\sigma_G^2} \mathbf{R}_G & \mathbf{0}_{m \times m} \\ \mathbf{0}_{n \times n} & \frac{1}{\sigma_G^2} \mathbf{R}_D \end{bmatrix}^{-1} \\ &= \begin{bmatrix} \frac{1}{\sigma_G^2} \mathbf{I}_{n \times n} & \mathbf{0}_{m \times m} \\ \mathbf{0}_{n \times n} & \frac{\sigma_D^2}{\sigma_G^2} \mathbf{I}_{m \times m} \end{bmatrix}^{-1} = \begin{bmatrix} \sigma_G^2 \mathbf{I}_{n \times n} & \mathbf{0}_{m \times m} \\ \mathbf{0}_{n \times n} & \frac{\sigma_G^2}{\sigma_D^2} \mathbf{I}_{m \times m} \end{bmatrix} \end{aligned} \quad (22)$$

The error covariance of the navigation solution obtained from the WLSM in the GPS/DME integration method can be represented in equation (23) (Kaplan and Hegarty, 2005, Won *et al.*, 2012).

$$\begin{aligned} \text{cov}(d\mathbf{x}) &= E[\Delta\hat{\mathbf{x}}\Delta\hat{\mathbf{x}}^T] \\ &= E\left[\left(\mathbf{H}^T \mathbf{W} \mathbf{H}\right)^{-1} \mathbf{H}^T \mathbf{W} \Delta\hat{\boldsymbol{\rho}} \Delta\hat{\boldsymbol{\rho}}^T \mathbf{W}^T \mathbf{H} \left(\mathbf{H}^T \mathbf{W} \mathbf{H}\right)^{-1}\right] \\ &= \left(\mathbf{H}^T \mathbf{W} \mathbf{H}\right)^{-1} \mathbf{H}^T \mathbf{W} E[\Delta\hat{\boldsymbol{\rho}} \Delta\hat{\boldsymbol{\rho}}^T] \mathbf{W}^T \mathbf{H} \left(\mathbf{H}^T \mathbf{W} \mathbf{H}\right)^{-1} \\ &= \sigma_G^2 \left(\mathbf{H}^T \mathbf{W} \mathbf{H}\right)^{-1} \mathbf{H}^T \mathbf{W} \mathbf{H} \left(\mathbf{H}^T \mathbf{W} \mathbf{H}\right)^{-1} \\ &= \sigma_G^2 \left(\mathbf{H}^T \mathbf{W} \mathbf{H}\right)^{-1} \\ &= \sigma_G^2 \mathbf{D}_w \end{aligned} \quad (23)$$

where \mathbf{D}_w denotes WDOP matrix. Therefore, altitude accuracy of the GPS/DME integration system can be estimated as equation (24) from error variance of the GPS measurements and WDOP matrix.

$$\hat{\sigma}_{GPS/DME \text{ Altitude}} = \sqrt{\sigma_G^2 \cdot D_{W33}} = \sigma_G \sqrt{D_{W33}} \quad (24)$$

If accuracy of the radio altimeter ($\hat{\sigma}_{RA\ Altitude}$) at the present altitude from the specification of the radio altimeter is compared with the accuracy of the GPS/DME integration system which is estimated from equation (24), use of the radio altimeter can be determined in the following manner.

if $\hat{\sigma}_{GPS/DME\ Altitude} > \hat{\sigma}_{RA\ Altitude}$
 use RA altitude output
else
 use GPS/DME altitude output

4. SIMULATION FOR PERFORMANCE EVALUATION

In order show effectiveness of the proposed method, simulations were performed. Figure 1 shows structure of the simulation. The motion trajectory generation part generates motion trajectory to the motion scenario. The GPS true range generation part and DME true range generation part generate true measurement from the vehicle trajectory, GPS satellite trajectory and position off the DME station. The raw measurement is generated by adding errors calculated from error specification to the true measurement. In the GPS/DME integrated navigation part, position and estimated position accuracy is generated using equation (17) and (24) from raw measurement. RA true altitude generation part and RA error generation part generates altitude and estimated altitude accuracy to the error specification of the radio altimeter. The GPS/DME/RA integrated navigation part determines use of the radio altimeter from the estimated accuracy of the altitude of the GPS/DME integration system and the estimated altitude accuracy of the radio altimeter.

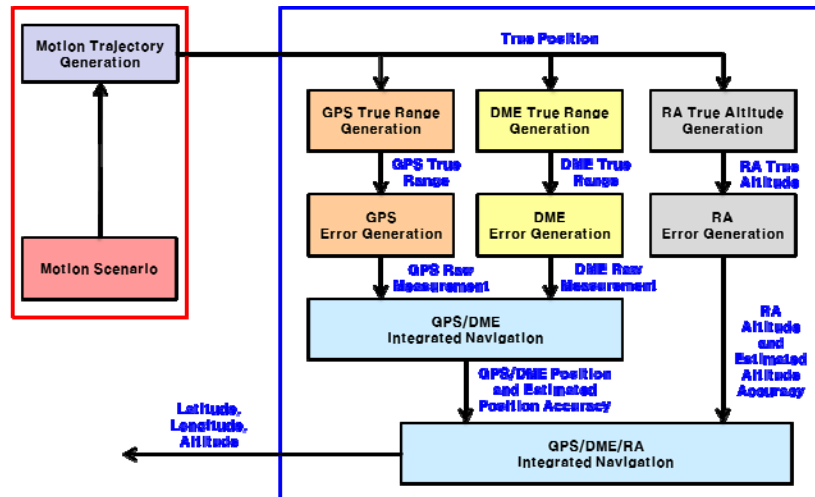


Figure 1. Simulation structure for performance evaluation

In the simulation, standard deviation of pseudo-range noise of the GPS signal was set to be 3 m and that of slant range noise of the DME signal 222 m. Error characteristic of the radio altimeter is given in Table 1 which is specification of Honeywell HG9550 radio altimeter (Honeywell, 2003).

Altitude	Error, Max
0 ~ 100 ft	± 2 ft
100 ~ 5000 ft	± 2 % of Altitude
5000 ~ 10,000 ft	± 100 ft
> 10,000 ft	± 1 % of Altitude

Table 1. Specification of Honeywell HG9550 radio altimeter

Figure 2 shows the reference trajectory for simulation and Figure 3 shows location of existing DME stations and motion trajectory of the vehicle to the ground. During the simulation time, five DME stations were selected among stations within DME signal arrival. The five stations form a geometrical arrangement which has minimum value of HDOP (Horizontal DOP).

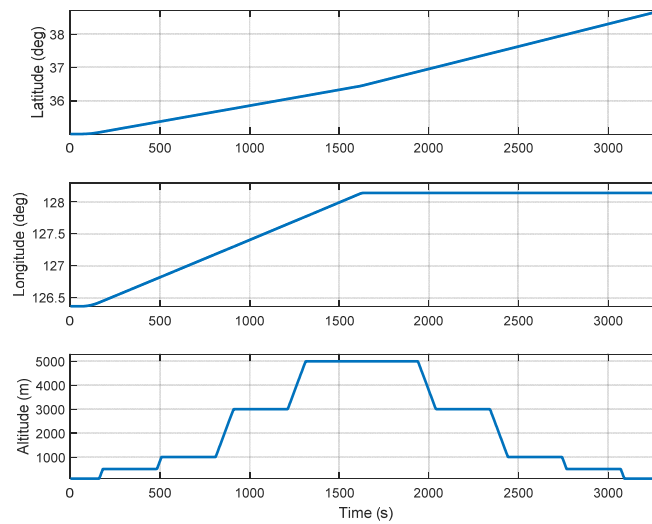


Figure 2. Reference trajectory for simulation

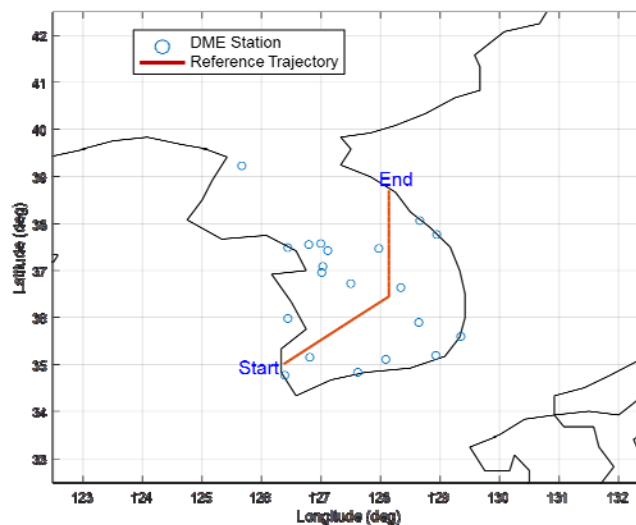


Figure 3. Location of DME station and ground track of motion trajectory

Figure 4 shows variation of the number of visible GPS satellites. First, GPS measurement was generated in the situation when the elevation mask angle was set to be at 0 degree. After then, in order to verify navigation performance of the case when the number of the GPS measurement is not enough, median value of the elevation of the satellites was calculated and measurements of the satellites which have larger than the median value were used in the simulation.

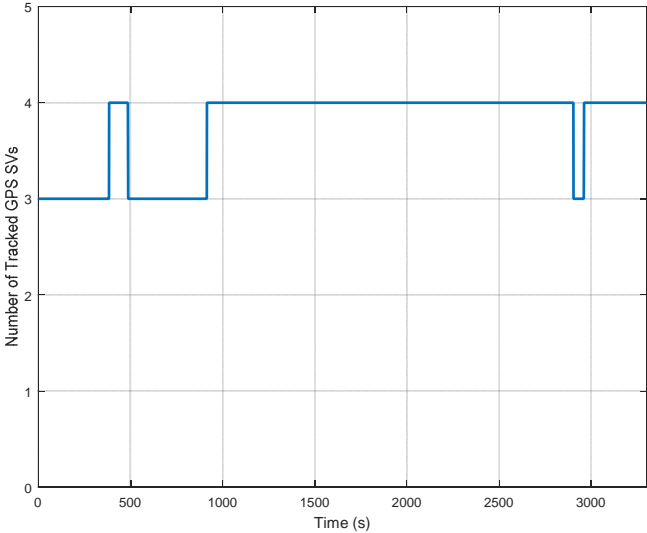


Figure 4. Number of visible GPS satellites

Figure 5 and 6 show RMS error and estimated value of navigation accuracy of the GPS/DME integration system and radio altimeter. It can be observed in Figure 5 that RMS error of the GPS/DME integrated navigation increases due to the large value of DOP in the interval where number of visible satellite are less than four. It can be seen that GPS measurement variance and estimated navigation accuracy from WDOP well reflect real RMS error. It can be observed in Figure 6 that altitude error increases as altitude becomes higher as the specification of the radio altimeter given in Table 1. It can be seen that the estimated altitude accuracy from error specification well reflects real RMS error.

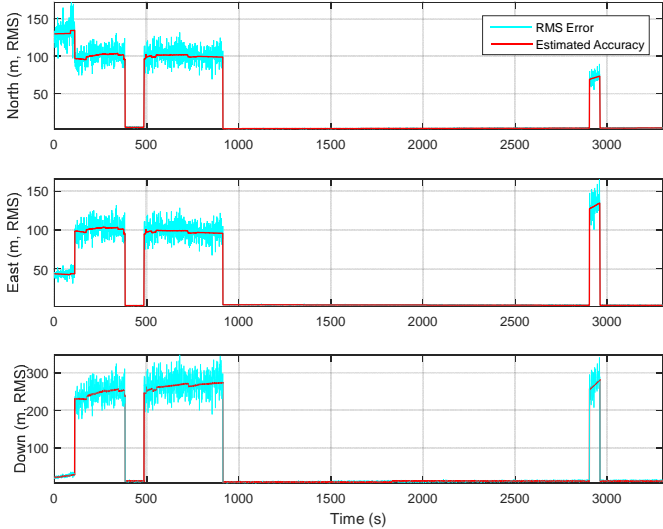


Figure 5. GPS/DME position RMS error with estimated position accuracy

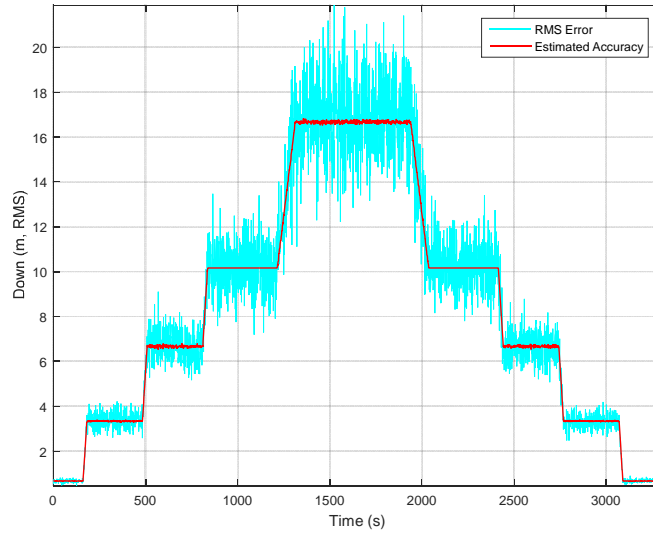


Figure 6. Radio altimeter altitude RMS error with estimated altitude accuracy

Figure 7 shows estimated altitude accuracy value comparison result of GPS/DME integration system and radio altimeter. When estimated value of the altitude accuracy of the GPS/DME is larger than that of radio altimeter, the altitude information of the radio altimeter is used in section 3. In Figure 8, altitude RMS errors are compared when the proposed algorithm is applied. It can be checked in Table 2 that more accurate altitude information can be provided when the radio altimeter is selectively used according to estimated navigation accuracy.

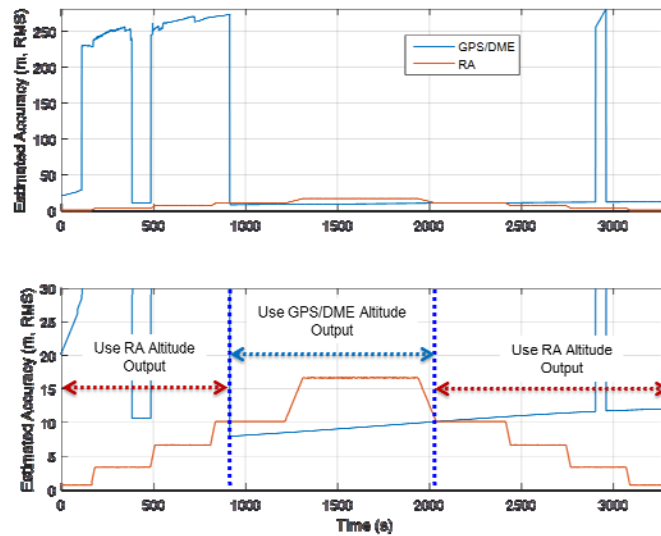


Figure 7. Selection of altitude output using estimated altitude accuracy

Source	Altitude Error (m, RMS)		
	Mean	Min	Max
GPS/DME	68.1	5.4	346.1
RA	8.5	0.5	21.9
GPS/DME/RA	6.6	0.5	13.5

Table 2. Altitude RMS error statistics of each navigation system

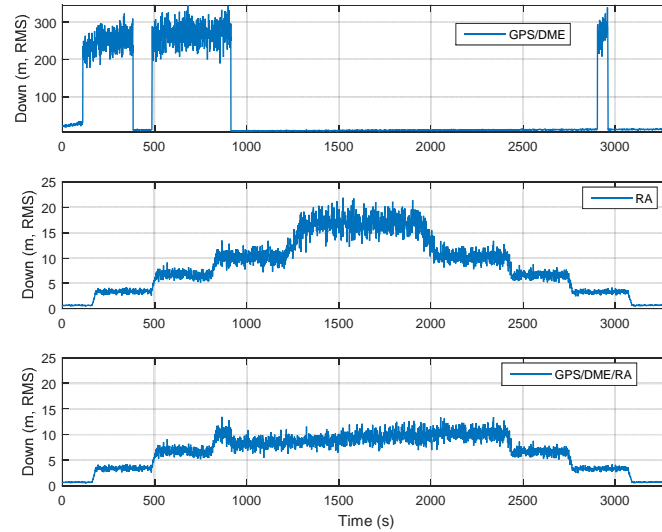


Figure 8. Altitude RMS errors of each navigation system

5. CONCLUDING REMARKS AND FURTHER STUDY

In this paper, an effective integrating method of the altitude information of the radio altimeter was proposed in the GPS/DME integrated navigation system. A navigation accuracy estimation method using WDOP in the GPS/DME integration system was presented. It has been shown through simulation that the proposed algorithm could have effectively determined use of a radio altimeter output under the condition that altitude of the vehicle and number of GPS measurements have varied.

The proposed algorithm can be extended to other ground based radio navigation systems such as eLoran, VOR, TACAN as further study.

ACKNOWLEDGEMENTS

This work has been supported by the National GNSS Research Centre program of Defense Acquisition Program Administration and Agency for Defence Development.

REFERENCES

- Bevly DM, Cobb S (2008), *GNSS for Vehicle Control*, Artech House, Boston
- Blanchard RL (1971) A new algorithm for computing inertial altitude and vertical velocity, *IEEE Transactions on Aerospace and Electronic Systems* 7(6): 1143-1146.
- FAA, (2014) NextGen Implementation Plan, Washington, DC, Available: http://www.faa.gov/nextgen/library/media/nextgen_implementation_plan_2014.pdf (accessed June 26, 2015)
- Gebre-Egziabher D (2004) Design and performance analysis of a low-cost aided dead reckoning navigator, *Ph.D. Thesis*, The Department of Aeronautics and Astronautics, Stanford University, Stanford
- Hofmann-Wellenhof B, Lichtenegger H, Collins J (1994) *Global Positioning System: Theory and Practice* (third, revised edition), Springer-Verlag, New York

- Honeywell (2003) *Datasheet for HG9550 Radar Altimeter System*, Honeywell Inc., Minneapolis
- Kaplan E, Hegarty C (eds) (2005) *Understanding GPS: principles and applications* (second edition), Artech House, Boston
- Kayton M, Fried WR (1997) *Avionics Navigation Systems* (second edition), John Wiley & Sons, New York
- Langley RB (1999) Dilution of precision, *GPS world* 10(5), 52-59.
- Leick A (1995) *GPS satellite surveying* (second edition), John Wiley & Sons, New York
- Misra P, Enge P (2006), *Global Positioning System : Signals, Measurements, and Performance* (second edition), Ganga-Jamuna Press, Lincoln
- Perrotta G, Girolamo SD, Galati G, Scarda S (1997) Transition phase a new navigation system based on a constellation of LEO satellites, *Mission Design & Implementation of Satellite Constellations: Proceedings of an International Workshop*, Toulouse, France, 179-189
- Titterton D, Weston JL (2004) *Strapdown inertial navigation technology* (second edition), AIAA, Reston
- Waite AH, Schmidt SJ (1962) Gross errors in height indication from pulsed radar altimeters operating over thick ice or snow, *Proceedings of the IRE* 50(6), 1515-1520.
- Won DH, Ahn J, Lee S-W, Lee J, Sung S, Park, H-W, Park J-P, Lee YJ (2012), Weighted DOP with consideration on elevation-dependent range errors of GNSS satellites, *IEEE Transactions on Instrumentation and Measurement* 61(12): 3241-3250
- Yoon J, Kwak HJ, Kim YH, Shin YJ, Yoo KJ, Yu MJ (2013) The performance analysis of an airborne radar altimeter based on simultaneously acquired LiDAR data, *Korean Journal of Remote Sensing* 29(1), 81-94